Modeling of special features of flow in a planar vortex chamber

D.V.VORONIN
Lavrentyev Institute of Hydrodynamics of SB RAS,
Lavrentyev str, 15, 630090 Novosibirsk
RUSSIA
Phone: +7 383 333 26 06;
Fax: +7 383 333 16 12;
E-mail: voron@hydro.nsc.ru, dvvoronin@bk.ru

Abstract. - The numerical calculations of the flowfield in a planar vortex chamber have been performed. The model is based on conservation laws of mass, momentum and energy for nonsteady two-dimensional compressible gas flow in case of swirl axial symmetry. The processes of viscosity, heat conductivity and turbulence have been taken into account. It was found that transition of kinetic energy of gas into heat due to processes of dissipation generates "hot spots" in boundary layers at the chamber walls. The gas temperature at the spots may exceed the temperature of gas ignition, while the surrounding regions remain still cold. It may be the reason of cold gas self-ignition observed in experiments.

Key words: - modeling, turbulence, compressible flows, hot spots, self-ignition

1 Introduction.

It is known that mixing of a fuel and oxidizer in a cold chamber leads to self-ignition for some particularly reactive fuel compositions, for example, for fluorine oxidizers [1]. The most frequently used mixtures of hydrocarbon fuels and hydrogen with air and oxygen ignite only as a result of additional external actions, such as rapid compression by a piston, compression by a shock wave, a spark, or a contact with a hot body. Spontaneous ignition of residual hydrocarbon fuels upon their contact with oxygen is known from the experience of exploitation of oxygen and high-pressure air tanks and pipelines [2]. In these cases, the phenomenon usually finds satisfactory explanation in the emergence of sparks due to accidental solid particles rubbing against the wall or by heating of some portions of the mixture upon its compression by a high-speed unsteady gas flow. For the first time spontaneous ignition of widely used fuel mixtures in a nonheated straight-flow chamber of the vortex type was obtained in paper [3]. The phenomenon had been observed accidentally in experiments on continuous detonation combustion of mixtures, where detonation was initiated by an electric discharge or by an explosion of a an electric microdetonator after the mixture fills the chamber. Examining the streak records of the processes it was found [3] that the glow in the chambers sometimes appears earlier than the triggering pulse. In subsequent experiments the regular self-ignition of hydrogen and kerosene was registered upon their mixing with oxygen-enriched air in a straight-flow vortex chamber. The nature of the ignition observed remained unclear.

The present paper devoted to numerical calculations of the flowfield in planar vortex chamber. The determination of non-stationary fields of main thermodynamic parameters allows to find possible regions of gas self-ignition. The geometry and main physical characteristics correspond to experimental data [3].

2 Problem Formulation

Let's consider a planar-radial circular chamber (Fig. 1). The chamber has axial symmetry form, where line A is a symmetry axis. The inner volume has the form of a disc of diameter $d_1 = 204$ mm and length $H = 15$ mm. The central outlet in one radial wall had a length $H_1 = 42$ mm and served to exhaust the products into atmosphere. The outlet diameter d_2 was equal to 40 mm. Gas components were fed into the chamber through circular inlet surface B (separating the chamber from the receiver) at an angle of 45^0 to the surface. The angle ensured rotational motion of the gas mixture in the chamber. The form and parameters of the chamber correspond to the experimental facility [3].

At the time $t = 0$, the entire chamber is filled by air of density ρ_0 and pressure p_0. At $t > 0$, the

tangential injection of air begins from the cylindrical wall $r = r_1$ (the inlet surface B). It is required to find the values of velocity, pressure, density and temperature of the gas as functions of time.

Unsteady motion of viscid compressible turbulent fluid was described by Reynolds equations [4]:

$$\frac{\partial Q}{\partial t} + \frac{\partial U}{\partial r} + \frac{\partial F}{\partial z} = G,$$

(1)

where r, z – radial and axial (along symmetry axis) cylindrical coordinates. The vectors Q, U, F, G are defined by the equations

$$Q = \begin{pmatrix} r\rho \\ r\rho u_r \\ r\rho u_\theta \\ r\rho u_z \\ rE \end{pmatrix}, \quad U = \begin{pmatrix} r\rho u_r \\ r(\rho u_r^2 + p - \tau_{11}) \\ r(\rho u_r u_\theta - \tau_{12}) \\ r(\rho u_r u_z - \tau_{13}) \\ r(E+p)u_r - r(u_r\tau_{11} + \\ u_\theta\tau_{12} + u_z\tau_{13} + q_r) \end{pmatrix},$$

$$F = \begin{pmatrix} r\rho u_z \\ r(\rho u_r u_z - \tau_{13}) \\ r(\rho u_\theta u_z - \tau_{23)} \\ r(\rho u_z^2 + p - \tau_{33}) \\ r(E+p)u_z - r(u_r\tau_{13} + u_\theta\tau_{23} \\ + u_z\tau_{33} + q_z) \end{pmatrix},$$

$$G = (0, \rho u_\theta^2 + p - \tau_{22}, -\rho u_r u_\theta + \tau_{12}, 0, 0),$$

here the components of the shear stress tensor have the form

$$\tau_{11} = (2/3)\mu_e(3e_{11} - divV), \quad \tau_{12} = \mu_e e_{12},$$
$$\tau_{22} = (2/3)\mu_e(3e_{22} - divV), \quad \tau_{13} = \mu_e e_{13},$$
$$\tau_{33} = (2/3)\mu_e(3e_{33} - divV), \quad \tau_{23} = \mu_e e_{23}.$$

The components of heat flux vector are

$$q_r = -\lambda_e \frac{\partial T}{\partial r}, \quad q_z = -\lambda_e \frac{\partial T}{\partial z}.$$

Here

$$e_{11} = \partial u_r / \partial r, e_{22} = u_r / r, e_{33} = \partial u_z / \partial z,$$
$$divV = e_{11} + e_{22} + e_{33}, e_{12} = \partial u_\theta / \partial r - u_\theta / r,$$
$$e_{13} = \partial u_r / \partial z + \partial u_z / \partial r,$$
$$e_{23} = \partial u_\theta / \partial z, E = \rho(e + q^2 / 2),$$
$$e = p /((\gamma - 1)\rho), q^2 = u_r^2 + u_\theta^2 + u_z^2,$$

the velocity vector has radial u_r, circumferential u_θ and axial u_z components; p, ρ, T and $\gamma = c_{p,1}/c_{v,1}$ are the pressure, density, temperature and the ratio of specific heats, respectively; μ_e and λ_e are the effective viscosity and effective thermal conductivity of the gas. μ_e is a sum of molecular μ and turbulent μ_t viscosity, $\lambda_e = c_p(\mu / \Pr + \mu_t / \Pr_t)$, $\Pr$ and $\Pr_t$ are molecular and turbulent Prandtl numbers.

The law of Sazerland is used for the values of molecular viscosity

$$\frac{\mu}{\mu_*} = \left(\frac{T}{T_*}\right)^{3/2} \frac{T_* + S_0}{T + S_0}$$

where $\mu_* = 1.68 \times 10^{-5}$ kg/(m·s), $T_* = 273$ K, $S_0 = 110$ K for air.

The processes of turbulence were described according to k-ε model:

$$\frac{\partial \rho k}{\partial t} + (\rho v \cdot \nabla)k = \nabla\left[\left(\mu + \frac{\mu_t}{\sigma_k}\right)\nabla k\right] +$$
$$+ P^* - \rho\varepsilon,$$

$$\frac{\partial \rho \varepsilon}{\partial t} + (\rho v \cdot \nabla)\varepsilon = \nabla\left[\left(\mu + \frac{\mu_t}{\sigma_\varepsilon}\right)\nabla \varepsilon\right] +$$
$$+ \frac{\varepsilon}{k}\left(C_{\varepsilon 1}P^* - C_{\varepsilon 2}\rho\varepsilon\right).$$

with values $\sigma_k = 1.0$, $\sigma_\varepsilon = 1.3$, $C_{\varepsilon 1} = 1.44$, $C_{\varepsilon 2} = 1.92$. Here k is turbulence kinetic energy, ε is its rate of dissipation, term P^* represents the production of turbulence kinetic energy, $P^* = \mu_t S^2$, $S = \sqrt{e_{ij}e_{ij}}$.

Turbulent viscosity was defined according to Kolmogorov-Prandtl formula:

$$\mu_t = \frac{C_\mu \rho k^2}{\varepsilon}, \quad C_\mu = 0.09.$$

The following boundary conditions are imposed:

on the planar radial walls of the chamber ($z = 0, 0 < r < r_1$, and $z = H, r_2 < r < r_1, r_1 = d_1/2, r_2 = d_2/2$) the condition of gas adhesion $u_r = u_z = u_\theta = 0$ and constant gas temperature on it: $T = T_0$;

on the inlet surface B ($r = r_1$, $0 < z < H$) $p = p^*(r_1, z, t)$, $\rho = \rho^*(r_1, z, t)$, $u_z = 0$, $u_\theta = u^*_\theta (r_1, z, t)$, $u_r = u^*_r(r_1, z, t)$. Functions p^*, ρ^*, u^*_θ, u^*_r depend on the dynamics of air overflow from the collector to the chamber   and are defined according to [3];

at the exit ($z = H + H_1$, $0 < r < r_2$) the conditions of equality to zero of the first derivatives of the thermodynamic parameters with respect to z, are valid.

3 Numerical solution of the problem

The calculations were performed for the following initial values of air: $p_0 = 1$ bar, $\rho_0 = 0.1225$ kg/m^3, $\gamma = 1.4$, $u_{r0} = u_{z0} = u_{\theta 0} = 0$; initial values of air pressure p_r and density ρ_r in the receiver : $p_r/ p_0 = 10$, $\rho_r/\rho_0 = 10$.

The problem stated above, was solved numerically with the help of the method of large particles [5].

The initial stage of numerical simulations is presented in Fig. 2. Here $u = \sqrt{u_r^2 + u_\theta^2 + u_z^2}$. It could be seen that a compression wave starts to propagate from the inlet surface B to the symmetry axis A. The pressure amplitude in the wave is up to 5.92 bar. The flow friction at the chamber walls results in mass growing of gas at the walls due to processes of dissipation, and subsequent transition of gas kinetic energy into heat starts. The values of temperature in generated boundary layers is growing up to 770 K ($z = 0$), while in the center of the channel it is equal to 520 K (at the same r and z = H/2).

The subsequent stage of the processes is presented in Fig. 3. The compression wave continues to propagate nearly at the same amplitude. The sizes of hot boundary layers are growing along with temperature values in them. The giant vortex is generated in the chamber at the walls. Its axes is the axes of symmetry A. The vortex is gradually coming down to the axes A. In recent simulations the initial pressure in the receiver $p_r = 10$ bar. In the experiments [3] it may be up to 100 bar. Then the temperature in the boundary layers (in the vortex) exceeds the ignition temperature $T_{ig} = 1200$ K. That results in self-ignition of gas in a whole volume observed in the experiments [3].

When the vortex comes down to the axes A, and gas masses collide (Fig. 4), the temperature amplitude reaches the value of 1480 K, that

initiates the processes of gas self-ignition even at present $p_r = 10$ bar. But the maximum of temperature takes place not at the axes of symmetry A but in the heated spot at the chamber corner ($r = r_2$, $z = H$), where the boundary layer tearing off from the chamber walls occurs.

Interaction of the heated spot with reflected shock waves (from the symmetry axes A) and gas acceleration in the spot (due to rarefaction wave) from the outlet surface result in subsequent temperature growth. At the course of time the temperature values in the spot exceed 2000 K (Fig. 5).

Dynamics of the maximum values of gas temperature we can see in Fig. 6. The dotted line in the figure corresponds to the value of ignition temperature T_{ig}. We can determine six stages of the processes. The initial stage 1 is a temperature growth from 300 K to 800 K, when the shock wave starts to propagate from the receiver to the chamber through the inlet surface B. The stagnation period 2 corresponds to the shock wave propagation to the center of the chamber (the symmetry axes A). The temperature growth at the stage 3 is a result of shock waves collision at the symmetry axes A. Here the gas temperature at the axes is increased up to 1500 K and exceeds the value of T_{ig}. That may result in gas self-ignition in the region. The interval 4 is the processes discharge in the direction of the outlet surface. The stage 5 is a temperature growth in the tearing off boundary layer at the chamber corner at its interaction with reflected shock wave. The temperature here exceeds here the value of 2100 K. The stage 6 lasts till rarefaction wave from the outlet surface appearance at the corner.

To appreciate the influence of turbulence on the gas self-ignition, the numerical simulations of laminar flow were performed on the base of Navier-Stokes equations (Fig. 7) at the same initial values of the problem parameters. It could be seen from the figure that for laminar flows the mixture self-ignition may occur as well. Although the maximum value of temperature in laminar hot spot T = 1370 K is significantly less than turbulent T = 2110 K at the same instant.

4 Conclusion

The numerical calculations of the flowfield in a planar vortex chamber on the base of Reynolds equations have been performed. The model is based on conservation laws of mass, momentum and energy for nonsteady two-dimensional compressible gas flow in case of swirl axial

symmetry. The processes of viscosity, heat conductivity and turbulence have been taken into account. It was found that transition of kinetic energy of gas into heat due to processes of dissipation generates "hot spots" in boundary layers at the chamber walls. The gas temperature at the spots may exceed the temperature of gas ignition, while the surrounding regions remain still cold. It may be the reason of cold gas self-ignition observed in experiments. The flow turbulence may play decisive role in possibility of gas self-ignition.

References.

[1] Mel'kunmov T.M., Melic-Pashaev N.I., Chistyakov P.G., Shuikov A.G., *Rocket engines*, Moscow, Mashinosnroenie, 1968.

[2] *Protection of labor in research institutions of the USSR Academie of Sciences*, Section Two: *Safety engineering during exploitation of tanks operating at high pressures,* Moscow, Nauka, 1972.

[3] Bykovskii F.A., Zhdan S.A., Mitrofanov V.V., Vedernikov E.F. Self-ignition and special features of flow in a planar vortex chamber, *Fizika gorenia i vzryva*, 2000, Vol. 35, No 6. pp. 26 – 41.

[4] Anderson D., Tannehill J., Pletcher R. *Computational fluid mechanics and heat transfer*, New York, Hemisphere, 1984.

[5] Belotsercovskii O.M., Davydov Yu.M. *Method of large particles in gas dynamics*, Moscow, Nauka, 1984.
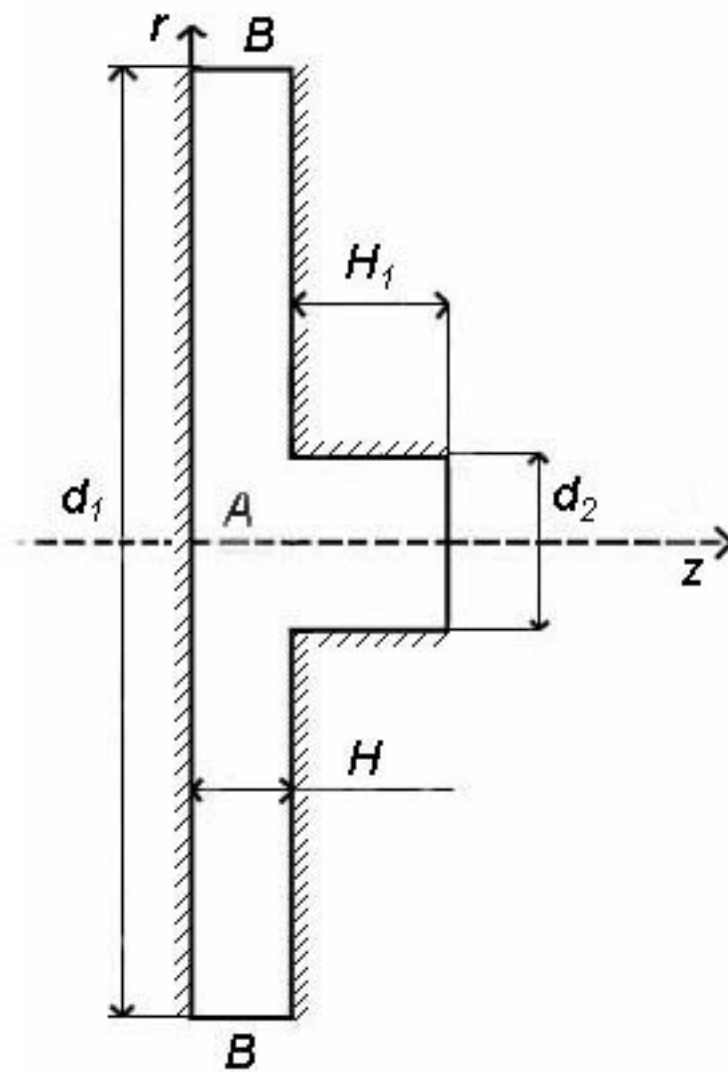
Fig. 1. The scheme of the vortex chamber.
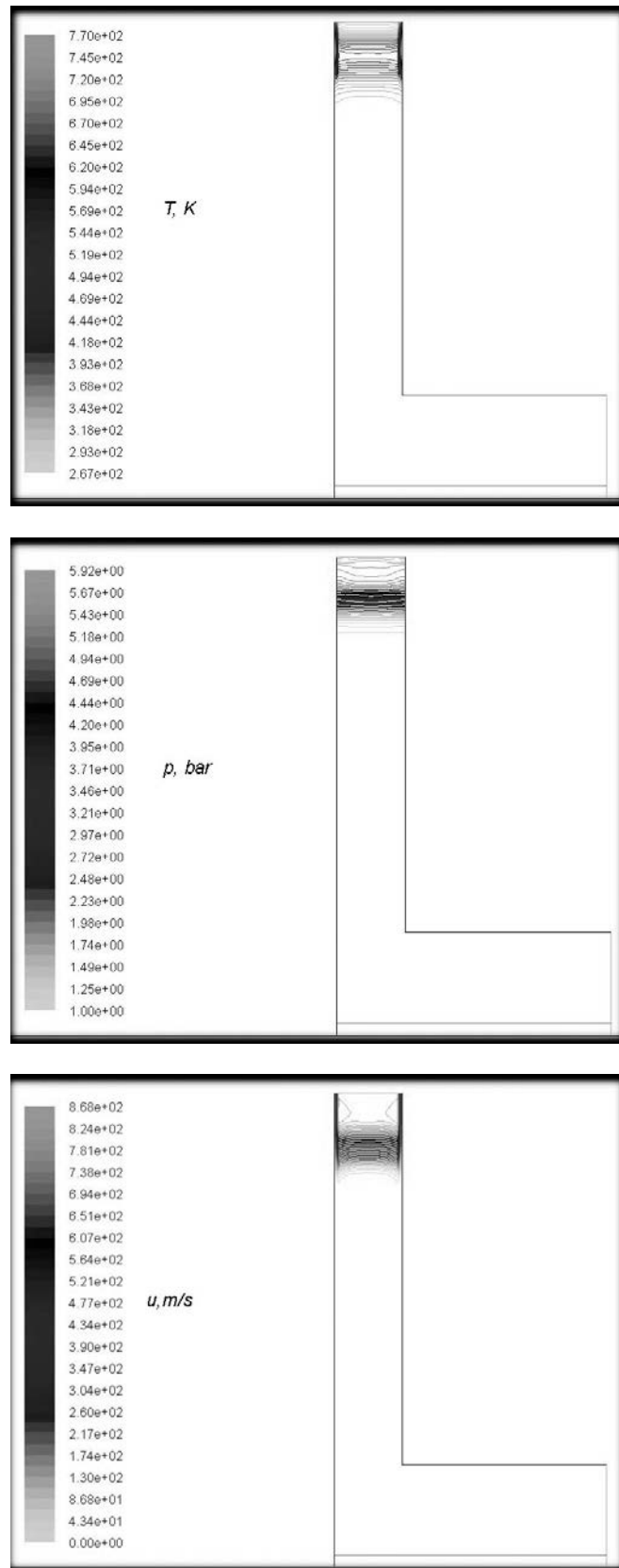
Fig.2. Flow field of the main thermodynamic parameters in the chamber at initial stage of the processes,
$t = 1.0 \cdot 10^{-4}$ s.
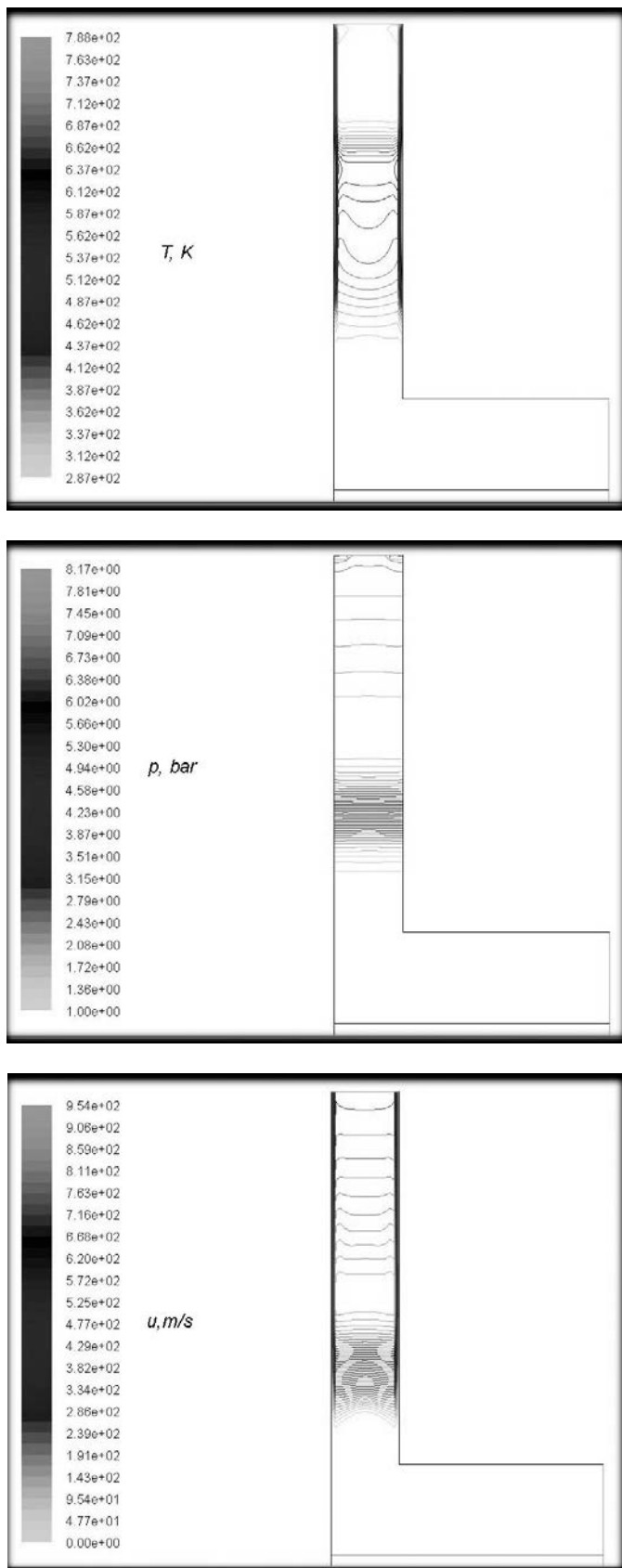
Fig. 3. The maps of the main thermodynamic parameters in the chamber at
$t = 5.0 \cdot 10^{-4}$ s.
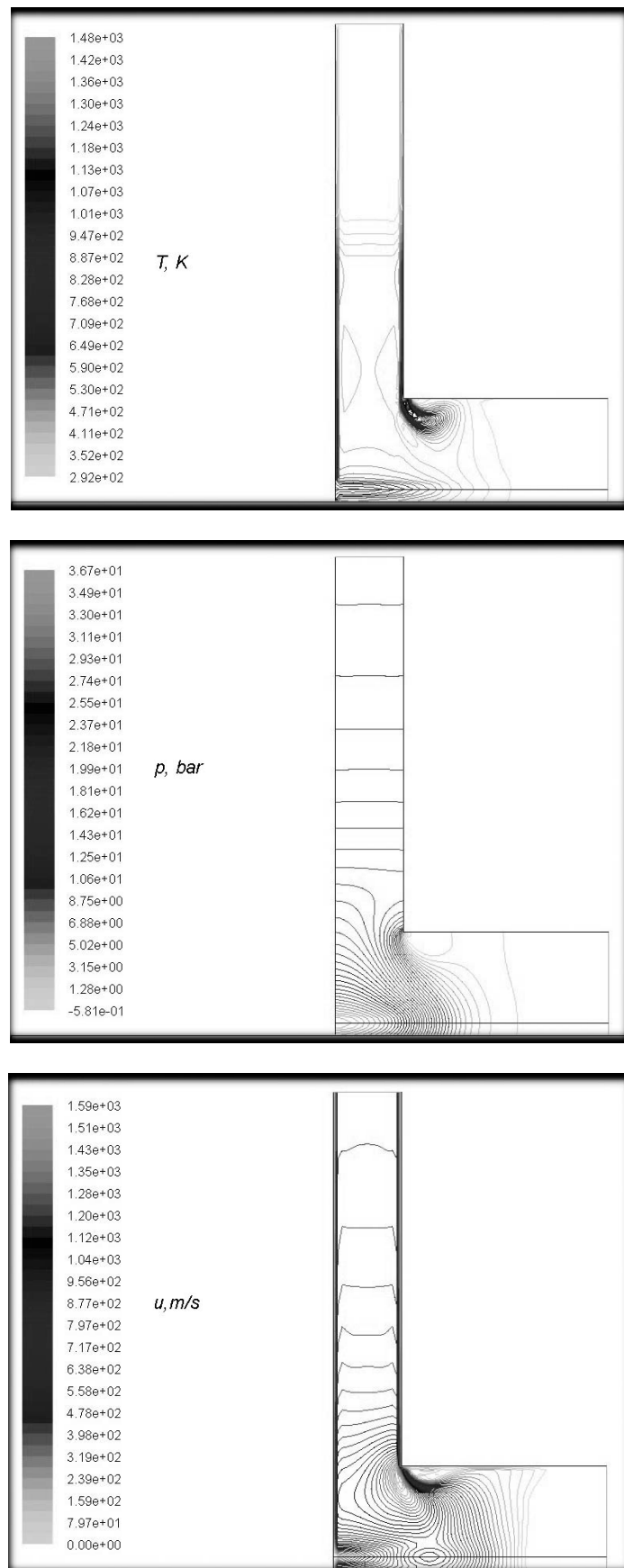
Fig. 4. The maps of the main thermodynamic parameters in the chamber at
$t = 9.0 \cdot 10^{-4}$ s.
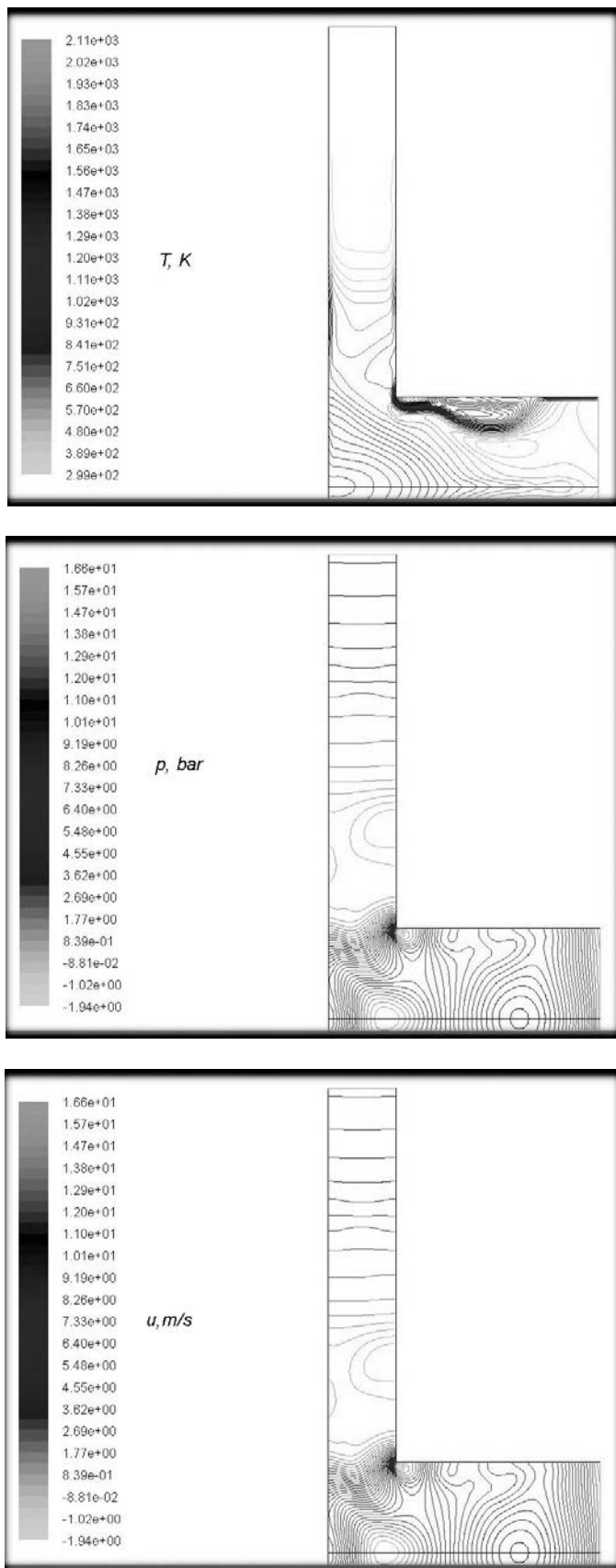
Fig. 5. The maps of the main thermodynamic parameters in the chamber at
$t = 1.4 \cdot 10^{-3}$ s.
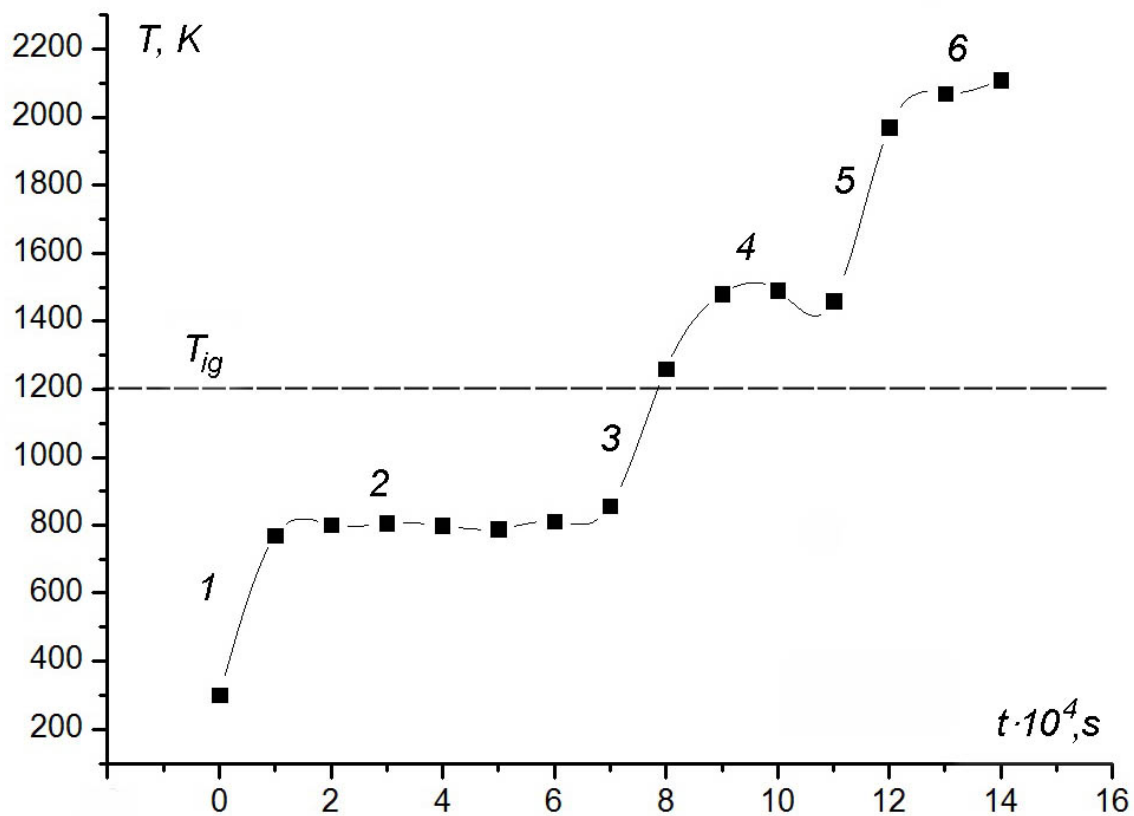
Fig. 6. Dynamics of the temperature maximum in the chamber.

$t = 1.0 \cdot 10^{-4}$ s.
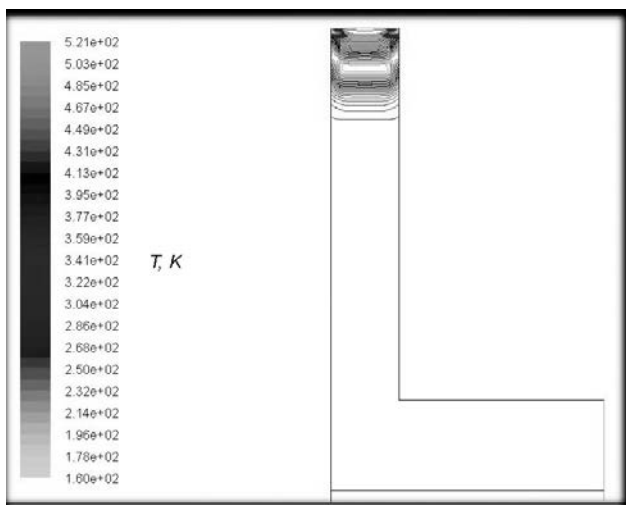
$t = 5.0 \cdot 10^{-4}$ s.
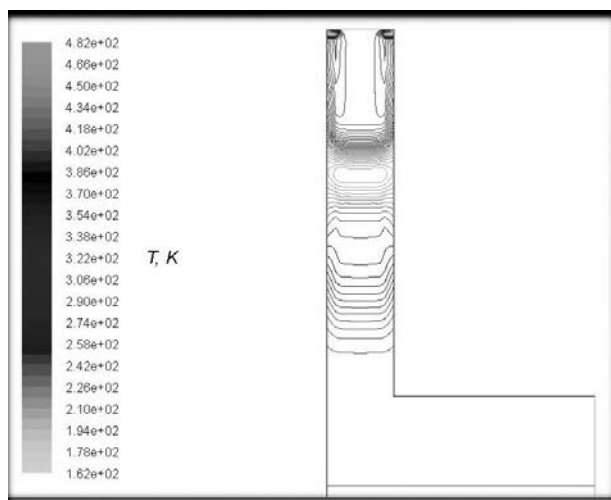
$t = 9.0 \cdot 10^{-4}$ s.
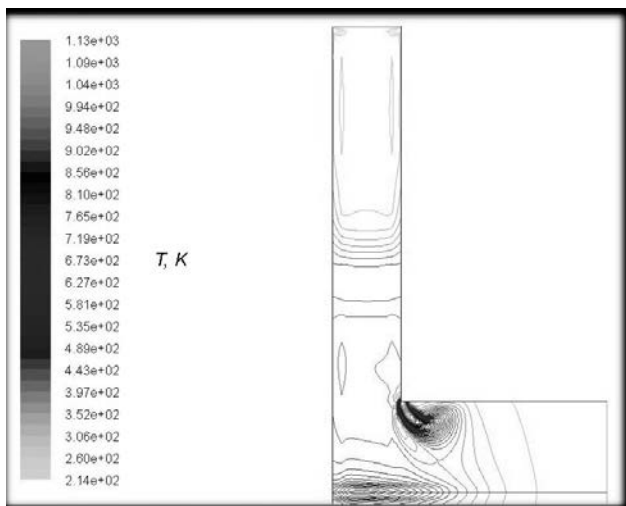
$t = 1.4 \cdot 10^{-3}$ s.
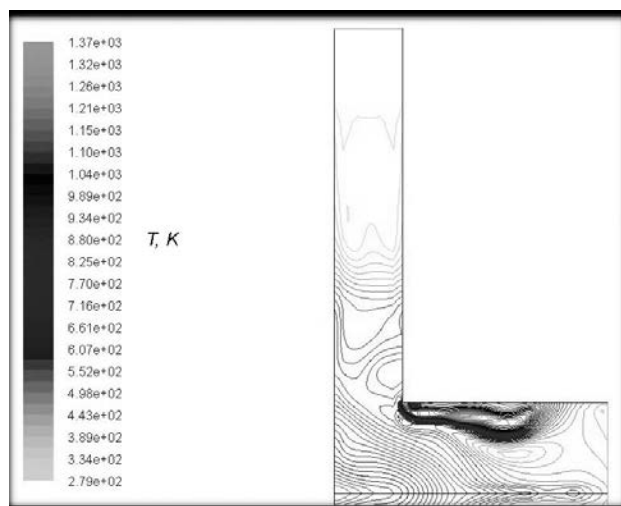
Fig. 7. The temperature maps in the chamber for laminar flow at
various instants.